# Effects of End-Group Balance on Melt-Phase Nylon 612 Polycondensation: Experimental Study and Mathematical Model

**ARTICLE** *in* INDUSTRIAL & ENGINEERING CHEMISTRY RESEARCH · DECEMBER 2004

Impact Factor: 2.59 · DOI: 10.1021/ie049474n



**4 AUTHORS**, INCLUDING:

Kimberley McAuley
Queen's University
**146** PUBLICATIONS **3,200** CITATIONS

SEE PROFILE

# Effects of End-Group Balance on Melt-Phase Nylon 612 Polycondensation: Experimental Study and Mathematical Model

**Wei Zheng,† Kim B. McAuley,* E. Keith Marchildon,† and K. Zhen Yao**

*Department of Chemical Engineering, Queen's University, Kingston, Ontario, Canada K7L 3N6*

The effects of end-group balance and moisture level on melt-phase polycondensation reactions were investigated using nylon 612. The polycondensation reaction was determined to be first-order in amine ends and first-order in carboxyl ends at the relatively high temperature (284 °C) and low water concentration conditions (0−0.002 mass fraction) studied, which are encountered in the later stages of nylon polymerization processes. Using data from this study and the nonisothermal data of Schaffer et al. (Chemical Pathways and Kinetics of the Later Stages of Nylon Polymerization Processes. Ph.D. Thesis, Queen's University, Kingston, Ontario, Canada, 2003; Experimental Study and Modeling of Nylon Polycondensation in the Melt Phase. *Ind. Eng. Chem. Res.* **2003**, *42*, 2946), a mathematical model was developed that can accurately describe changes in both the polyamidation reaction rate and the apparent equilibrium constant, with changing water concentration and temperature.

## Introduction

Nylons are important commercial polymers that are produced through reversible polycondensation reactions between amine and carboxyl end groups. The forward reaction is a polyamidation reaction, and the reverse reaction is a hydrolysis reaction:

$$-\mathrm{COOH} + -\mathrm{H_2N} \rightleftharpoons -\mathrm{CONH}- + \mathrm{H_2O}$$

Published research on the kinetics of the previous reaction is somewhat contradictory. Some researchers contend that the reaction obeys second-order kinetics (first order in both amine and acid end groups).[3−8] Several studies of polyamidation, under conditions where the end-group concentrations are relatively low (i.e., conversions above 90%), indicate that a carboxyl-catalyzed third-order reaction assumes increasing importance and becomes predominant. So, other researchers[9−13] have suggested that there is a shift from second- to third-order kinetics, involving catalysis by the carboxylic acid end group, at low water contents and high conversions. In addition, a study of the hydrolysis of amides at 220 °C in near-neutral buffered solutions has shown that this reaction is carboxyl-catalyzed. Therefore, some researchers have assumed third-order kinetics (first order in amine ends and second order in carboxyl ends) over the entire water concentration range.[14]

The majority of experimental studies on nylon kinetics and equilibrium in the open literature focus on nylon 6[3,15−24] and nylon 66.[25,26] Both nylon 6 and nylon 66 are commercially important nylon products, but they are not ideal materials for studying polycondensation kinetics. During nylon 6 polymerization, ring opening of caprolactam and polyaddition reactions occur in addition to the polycondensation reaction, complicating the study of amidation kinetics. In the production of nylon 66, thermal degradation reactions, resulting from the cyclization of adipic acid segments,[27−30] influence the concentrations of end groups, thereby preventing accurate estimation of the rate and equilibrium constants for polycondensation.

In this study, nylon 612, a commercial polymer made from dodecanedioc acid (DDDA) and hexamethylenediamine (HMD), is used to study nylon polyamidation kinetics. Nylon 612 is more thermally stable than nylon 66 because it does not have adipic acid segments in the polymer chains. Unlike nylon 6, ring-opening and polyaddition reactions do not occur. As in previous studies, we assume that the lengths of the aliphatic portions of the polymer repeat units do not affect the end-group reactivity,[5−8,31,32] so that the kinetics of the polycondensation reactions from nylon 612 are comparable with the kinetics for other aliphatic polyamides.

Most of experimental studies on nylon kinetics and equilibrium in the open literature focus on conditions of high water content and low temperature, which are encountered early in the polyamidation process;[3,6,26] relatively few data have been reported for conditions of low water content and high temperature,[1,2,25] which are present in the final stages of industrial nylon production processes. A better understanding of this stage is very important for industrial reactor design, product quality control, and optimization of process operating conditions. The objectives of this study are to use nylon 612 to examine the effects of end-group balance on the kinetics of the polycondensation reaction, to distinguish whether the polycondensation reaction obeys second- or third-order kinetics in the later stages of polyamide production, and to estimate the rate and equilibrium constants of the polycondensation reaction at high temperatures and low water contents.

## Experiments

Figure 1 shows a schematic diagram of the batch reactor system. The reactor itself is based on the design of finisher reactors described in several patents[33−36] that are used industrially as the final stage of continuous nylon 66 polymerization processes. The reactor vessel is a 5-L stainless steel stirred tank, with two intermeshing helical impellers entering from the bottom. The

* To whom correspondence should be addressed.

† Current address: Research and Business Develop Centre, DuPont Canada Inc., Kingston, Ontario, Canada K7L 5A5.

10.1021/ie049474n CCC: $30.25 
Published on Web 12/17/2004

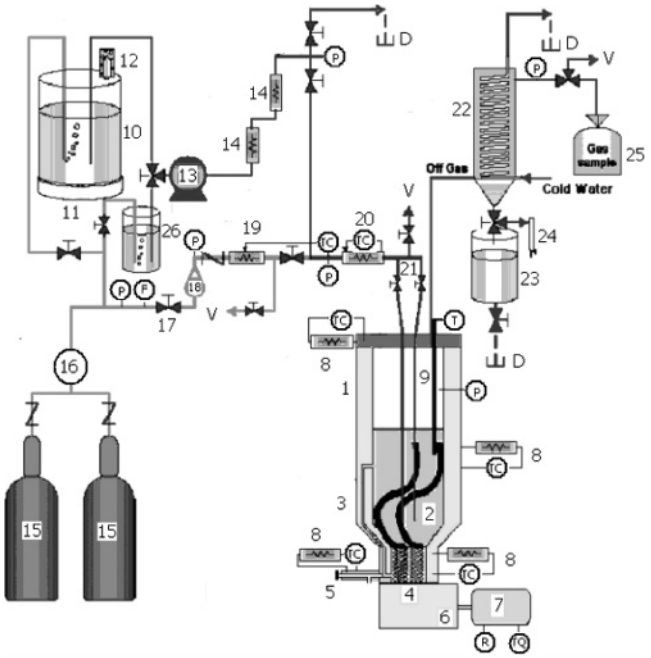


**Figure 1.** Schematic drawing of the experimental apparatus: (1) reactor vessel; (2) impellers; (3) recirculation channel; (4) extruder section; (5) sample valve; (6) gearbox; (7) motor and drive; (8) reactor heating zones; (9) melt RTD; (10) water tank; (11) scale; (12) water seal; (13) pump; (14) steam-generating heaters; (15) $N_2$ cylinders; (16) regulator; (17) $N_2$ metering valve; (18) rotameter; (19) $N_2$ preheater; (20) final heater; (21) sparger tubes; (22) glass coil condenser; (23) condensate tank; (24) buret; (25) gas sampling bag; (26) HMD water solution tank; (P) pressure gauge; (T) temperature sensor; (TC) temperature controller; (F) mass flowmeter; (R) rpm sensor; (TQ) torque sensor; (D) drain; (V) vent.

reactor has a figure-eight cross section to accommodate the range of motion of the impellers and to give a close clearance between the vessel wall and the impellers. A twin-screw extruder section, at the bottom of the vessel, pumps the polymer melt through a recirculation channel bored through the wall of the vessel and back into the reactor interior. A sample valve connects to the recirculation channel so that multiple samples of the polymer can be taken during each experimental run. The mixing features of the reactor and its detailed internal structure were described by Schaffer et al.[37]

To adjust the water content in the molten polymer, steam is generated, mixed with nitrogen in a desired ratio, and delivered to the reactor vessel as a preheated sparge gas. The flow rate, composition, and temperature of the sparge gas are regulated. After the sparge gas bubbles through the polymer melt, the off-gas enters a water-cooled glass coil condenser. The condensate from the off-gas is collected in a 4-L tank, and its flow rate is estimated by measuring the time to fill a 10-mL buret.

All experimental runs were conducted using additive-free nylon 612 polymer pellets supplied by DuPont Canada. This polyamide had a carboxyl end-group concentration that was 68 mol $Mg^{-1}$ higher than the amine end-group concentration. In previous experiments, conducted by Schaffer et al.,[1,2] samples of this polymer were polymerized using a mixed steam-and-nitrogen sparge gas over a range of temperatures (263−289 °C) without adjusting the difference in the end-group concentrations (i.e., as polymerization occurred, the carboxyl and amine end-group concentrations rose and fell together, but the difference between the end-group concentrations was the same for all of the experiments). One objective in this work is to study the polyamidation kinetics using polymer samples with differences of end groups (carboxyl minus amine) ranging from ~0 to 200 mol $Mg^{-1}$ so that better information about the reaction order can be obtained.

For runs in which additional carboxyl groups in the polymer melt were desired, compared with those in the initial nylon 612 polymer pellets, the DDDA powder was mixed with the nylon 612 pellets before they were added to the reactor. Subsequently, DDDA reacted with the polymer by transamidation reactions, increasing the carboxyl end-group concentration of the molten polyamide. For runs in which additional amine groups were desired, a 50 wt % HMD−water solution was vaporized and bubbled through the melt via the sparge tubes. Some of the HMD was absorbed by the molten polymer phase and reacted with the polymer to change the end-group balance, while some of the HMD exited the reactor as a vapor and entered the water-cooled glass coil condenser. Condensate samples were taken and analyzed so that the amount of HMD that stayed in the melt phase could be estimated.

During each experimental run, approximately 2270 g of preweighed polymer pellets was charged to the reactor. The vessel was sealed and thoroughly purged with nitrogen to remove residual air. After the temperature reached the desired value of 284 °C, the sparge-gas composition was switched to pure steam, and the first sample was taken. A total of 1 or 2 h was allowed to elapse so that the polymer could reach phase and reaction equilibrium with the steam. Several polymer samples were then taken to permit verification of steady-state equilibrium conditions by subsequent analyses. The concentration of water in the sparge gas was then reduced by starting the flow of nitrogen and lowering the water pump rate, allowing the polymer to reequilibrate while more polymer samples were taken. Pure steam conditions were then reestablished, allowing the polymer to equilibrate a third time while samples were taken. Analyses of amine and carboxyl end-group concentrations were performed for each polymer sample using titration methods similar to those outlined by Sibila et al.[38]

## Experimental Results

Three experimental runs were performed at 284 °C using different initial end-group concentrations. The initial end-group concentrations for these three runs were $[C]_{initial}$ = 133 mol $Mg^{-1}$, $[A]_{initial}$ = 25 mol $Mg^{-1}$; $[C]_{initial}$ = 212 mol $Mg^{-1}$, $[A]_{initial}$ = 13 mol $Mg^{-1}$; and $[C]_{initial}$ = 53 mol $Mg^{-1}$, $[A]_{initial}$ = 49 mol $Mg^{-1}$, respectively. The water partial pressure in the sparge gas employed in this study was changed between 20.7 and 101.3 kPa. These experimental conditions correspond to relatively high temperatures and low melt-phase water concentrations, in comparison with most previous studies of nylon polycondensation. The experimental end-group data are plotted versus reaction time in Figures 2−4. The less-precise nature of the acid end-group concentration measurements is reflected by the greater degree of scatter in these data than in the amine end-group concentration data.

In the initial stages of each experimental run, equilibrium was established under a steam atmosphere. Decreasing the water partial pressure, $P_w$, in the sparge gas from the initial condition caused the water concentration in the melt to decrease rapidly so that the polycondensation reaction rate became faster than the

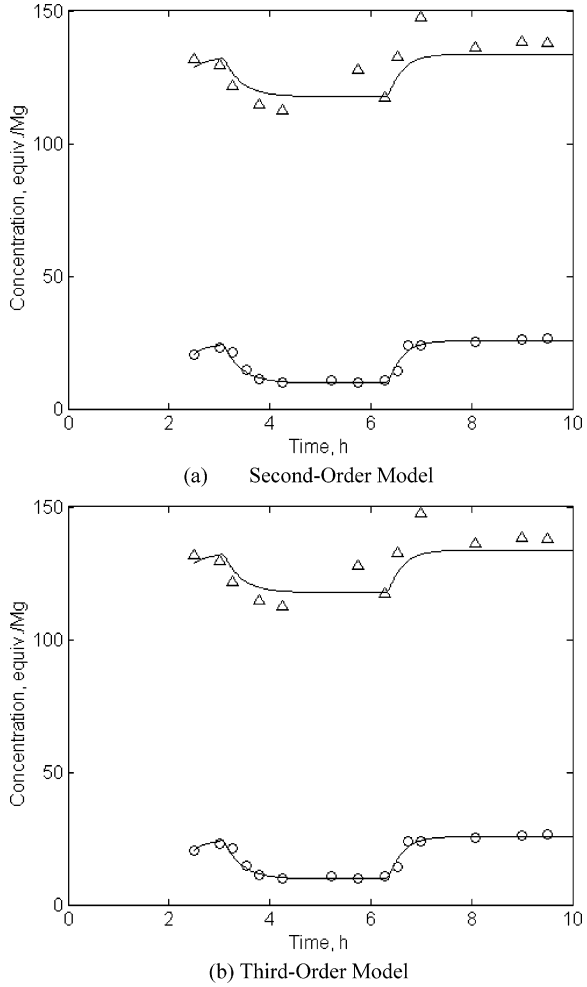


**Figure 2.** Experimental end-group data and comparison with second-order (a) and third-order (b) model predictions for run at 284 °C with [C] − [A] = 108 mol $Mg^{-1}$: (△) measured [C]; (○) measured [A]; (—) model.

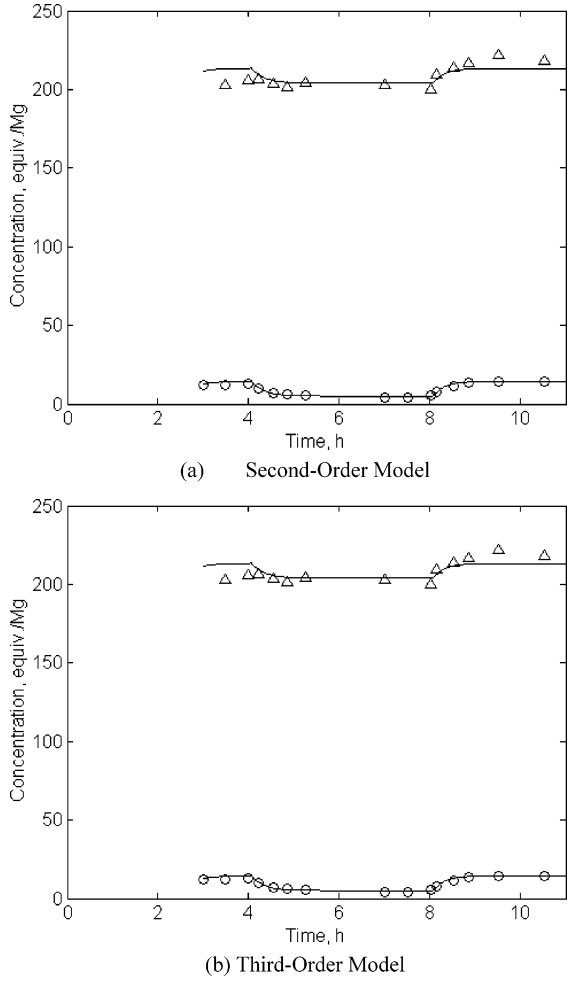


**Figure 3.** Experimental end-group data and comparison with second-order (a) and third-order (b) model predictions for run at 284 °C with [C] − [A] = 199 mol $Mg^{-1}$: (△) measured [C]; (○) measured [A]; (—) model.

hydrolysis reaction rate. Thus, the end-group concentrations decreased as amide linkages were formed. Equilibrium was reestablished at these conditions of lower water concentration. Then $P_w$ was increased, and the melt-phase water concentration increased again. Under these higher water conditions, the hydrolysis reaction rate was faster than the polycondensation reaction rate, leading to a net hydrolysis of amide linkages. The end-group concentrations increased until equilibrium was reestablished under conditions similar to those at the beginning of the experimental run.

Sufficient time elapsed so that reaction equilibrium was established after each step change in $P_w$ in the first two experiments (Figures 2 and 3) but not at the low water concentration conditions in the third run (Figure 4). Based on the equilibrium data from the first two runs, the apparent equilibrium constant[1,2]

$$K_a = \frac{[L]_{eq}[W]_{eq}}{[C]_{eq}[A]_{eq}} \quad (1)$$

was not affected by the end-group balance. $[L_{eq}]$ and $[W]_{eq}$ are the equilibrium concentrations of amide links and water in the polymer melt, and $[C]_{eq}$ and $[A]_{eq}$ are the corresponding carboxyl and amine end-group concentrations, respectively. However, the observed end-group concentrations at equilibrium, within each run, confirmed[1,2] that the water content can influence the apparent equilibrium constant significantly in this low-water-content operating regime, agreeing with Giori and Hayes' results.[22] Giori and Hayes observed that the apparent equilibrium constant decreased with decreasing water content in the water-content range below 2 wt %.

In Figures 2−4, it is apparent that both [A] and [C] behave similarly, increasing and decreasing in parallel, as is expected in a system where thermal degradation of the polymer is not occurring to any appreciable extent. This was not the case in several other studies,[1,39−42] where nylon 66 was held for extended time periods under similar conditions of temperature and water content; considerable increases in [A] and decreases in [C] were observed as a result of thermal degradation. These results confirm that nylon 612 is more thermally stable than nylon 66. Furthermore, only very small changes in the reactor drive torque were observed throughout each run, and these changes were attributable to viscosity changes due to changes in the degree of polymerization. In previous thermal degradation experiments with nylon 66,[1] when the polymer became appreciably branched or gelled, the drive torque increased substantially as a result of increasing the viscosity of the polymer melt.

To save on analytical costs, less-precise carboxyl end-group concentrations were measured for only some of

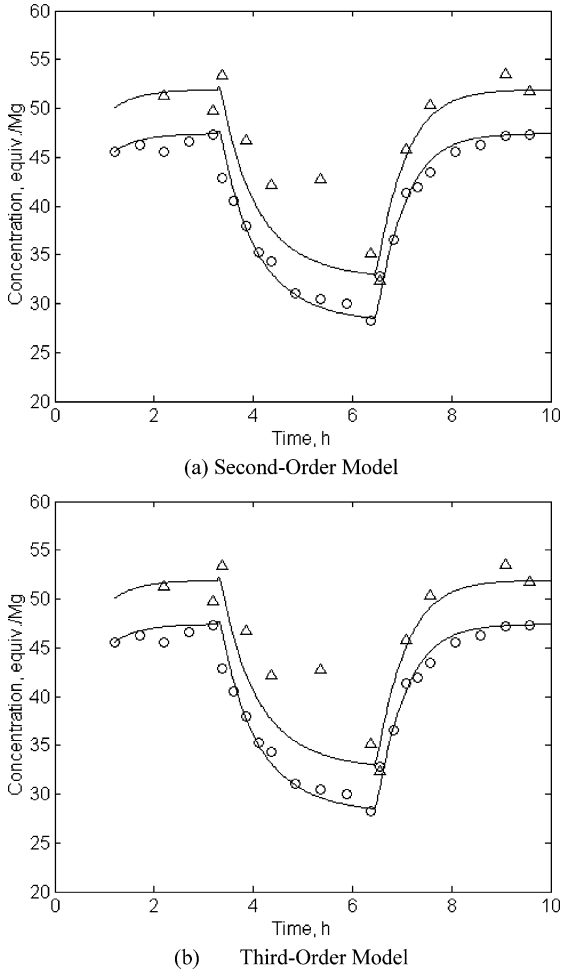


**Figure 4.** Experimental end-group data and comparison with second-order (a) and third-order (b) model predictions for run at 284 °C with [C] − [A] = 4.5 mol $Mg^{-1}$: (△) measured [C]; (○) measured [A]; (—) model.

the samples, whereas more-precise amine end-group concentration measurements were made for every sample. Results from the samples with both measurements were used to determine that the differences between the carboxyl and amine end-group concentrations for the three runs were 108 mol $Mg^{-1}$ (Figure 2), 199 mol $Mg^{-1}$ (Figure 3), and 4.5 mol $Mg^{-1}$ (Figure 4). In recent experiments by Schaffer et al.,[2] in which we used the same nylon 612 starting polymer, all runs had the same difference of ends, near 68 mol $mg^{-1}$. The results from the current experiments confirmed that we are able to make significant adjustments to the end-group balance of the original nylon 612 by either adding adipic acid powder (before melting the pellets) or sparging a HMD/steam mixture through the melt at the beginning of the experiment, depending on whether a larger or smaller difference of ends is required.

## Reaction-Order Determination

To determine the kinetic rate constant for the forward amidation reaction under different reaction-order assumptions, it is necessary to determine the apparent equilibrium constant (eq 1). Measurements of $[C]_{eq}$ and $[A_{eq}]$ are available from the steady-state portions of Figures 2−4. Unfortunately, however, $[W]_{eq}$, the water content of the nylon melt at both chemical and vapor−liquid equilibrium, is difficult to measure reproducibly (particularly at low water contents) because hygroscopic nylon samples absorb water from the atmosphere during sampling and sample handling.[1,2] Fortunately, $[W]_{eq}$ can be estimated for nylon 612 samples using a correlation[43] based on the Flory−Huggins theory:

$$[W]_{eq} = 5.55 \times 10^4 (P_w/P_w^{sat}) \exp(-9.624 + 3613/T) \quad (2)$$

where $P_w$ is the partial pressure of water in the vapor phase in equilibrium with the molten polymer and $P_w^{sat}$ is the saturation pressure of pure water at the temperature of melt. $P_w^{sat}$ can be calculated from the Wagner equation.[42]

$$\ln(P_w^{sat}/P_c) = [-7.77224(1 - T/T_c) + 1.45684(1 - T/T_c)^{1.5} - 2.71492(1 - T/T_c)^3 - 1.41336(1 - T/T_c)^6]/(T/T_c) \quad (3)$$

$P_c$ and $T_c$ are the critical pressure and temperature of water.

The net polycondensation rate in the batch reactor can be expressed by eq 4, and the rate of change of the water content in the melt phase is described by eq 5,

$$\frac{d[L]}{dt} = -\frac{d[A]}{dt} = -\frac{d[C]}{dt} = k_p[C]^X\left([C][A] - \frac{[L][W]}{K_a}\right) \quad (4)$$

$$\frac{d[W]}{dt} = k_p[C]^X\left([C][A] - \frac{[L][W]}{K_a}\right) - k_m([W] - [W]_{eq}) \quad (5)$$

where the exponent $X$ is zero if the reaction is second order (first order in carboxyl ends and first order in amine ends) and unity if the reaction is third order (second order in carboxyl ends and first order in amine ends). $k_m$ in eq 5 is a volumetric mass-transfer coefficient (the product of the mass-transfer coefficient and the interfacial area per unit volume) for the transport of water between the melt and vapor phases. For our reactor system and operating conditions, it is appropriate to use $k_m$ = 24.3 $h^{-1}$, which was estimated by Schaffer et al.[1,2] in a previous study. [L], [C], [A], and [W] in eqs 4 and 5 are the instantaneous concentrations of amide links, carboxyl ends, amine ends, and water in the molten polymer, respectively. For nylon 612, [L] can be computed from a material balance.

$$[L] = \frac{10^6 - 115.15[C] - 58.10[A] - 18.02[W]}{155.23} \quad (6)$$

Note that the typical concentration units used in the nylon polymerization industry are mole equivalents per $10^6$ g of polymer. Equation 6 uses the molar masses of carboxyl ends, amine ends, water, and amide links (which are 115.15, 58.10, 18.02, and 155.23 g $mol^{-1}$, respectively) to compute [L], which is the number of moles of amide links in $10^6$ g of polymer.

Matlab was used to solve the differential equations (eqs 4 and 5) numerically. A fourth-order Runge−Kutta method was used with a fixed step size of 0.01 h. Reducing the step size had a negligible effect on the simulation results. Equation 4 was used to solve for both the amine and carboxyl end-group concentrations. The initial value used to solve for the amine end-group

**Table 1. Parameter Estimation Results for Second- and Third-Order Models Fitted Separately to Each Run**

| | | | measured $K_a$ | | | | | |
|---|---|---|---|---|---|---|---|---|
| $T$, °C | $[C]_{initial}$, mol $Mg^{-1}$ | [C] − [A], mol $Mg^{-1}$ | under steam | under $N_2$ | second-order $k_p$, Mg $mol^{-1}$ $h^{-1}$ | 95% CI (±) | third-order $k_p$, $Mg^2$ $mol^{-2}$ $h^{-1}$ | 95% CI (±) |
| 284 | 130 | 108 | 70 | 48 | $2.55 \times 10^{-2}$ | $1.01 \times 10^{-2}$ | $1.96 \times 10^{-4}$ | $0.77 \times 10^{-4}$ |
| 284 | 212 | 199 | 74 | 50 | $2.15 \times 10^{-2}$ | $1.38 \times 10^{-2}$ | $1.01 \times 10^{-4}$ | $0.64 \times 10^{-4}$ |
| 284 | 53 | 4.5 | 90 | 50 | $2.04 \times 10^{-2}$ | $0.26 \times 10^{-2}$ | $3.85 \times 10^{-4}$ | $0.49 \times 10^{-4}$ |

concentration profile was the measured value from the first sample. Because carboxyl end-group concentration measurements were noisier and were not available for the first sample in all runs, the initial condition used to simulate carboxyl end-group concentration profiles was the sum of the initial measured amine end-group concentration and the average difference of the ends for the particular run.

Because the [C] measurements are less reliable than the more-precise [A] measurements, weighted nonlinear least-squares regression was used to ensure that the parameter estimates are less influenced by measurements of [C] than [A]. In the objective function, $J$, for parameter estimation, the squared prediction errors for [A] and [C] were weighted by $1/\sigma_A^2$ and $1/\sigma_C^2$, respectively, which are the reciprocals of the respective measurement variances estimated from replicate analyses of previous polymer samples:

$$J = \sum_{j=1}^{n_A}\left[\frac{1}{\sigma_A^2}([A]_i - [\hat{A}]_i)\right]^2 + \sum_{l=1}^{n_C}\left[\frac{1}{\sigma_C^2}([C]_l - [\hat{C}]_l)\right]^2 \quad (7)$$

The standard deviations, $\sigma_A$ and $\sigma_C$, used in the objective function were 0.6 and 2.4 mol $Mg^{-1}$, respectively. $n_A$ and $n_C$ are the respective number of amine and carboxyl end-group samples, used for parameter estimation; $[\hat{A}]_i$ and $[\hat{C}]_l$ are the respective model predictions for amine and carboxyl end-group concentrations. Note that the estimates of $\sigma_A^2$ and $\sigma_C^2$ may be lower than the true variances for experimental replicates because they were determined from measurement errors alone rather than true experimental replicates. Also, this estimation approach neglects the correlation between the random errors in [A] and [C] for the same polymer sample, as well as any autocorrelation in residuals between subsequent measurements from the same run.

The polyamidation rate constant, $k_p$, was estimated for each of the three individual runs shown in Figures 2−4, first assuming second-order kinetics ($X = 0$) and then using third-order kinetics ($X = 1$). In these preliminary parameter estimation studies, the apparent equilibrium constant, $K_a$, during each step up or down in moisture level, was calculated using the measured equilibrium concentrations obtained at the end of the particular step so that $k_p$ was the only unknown parameter requiring estimation. The results of this parameter estimation study are shown in Table 1, and the corresponding simulation results are shown in Figures 2−4.

Comparing parts a and b of Figures 2−4 reveals that both the second- and third-order model formulations can fit the experimental data equally well when each run is fitted separately. When the second-order formulation is used, the polyamidation rate constant estimates have almost the same value, with 95% confidence intervals that overlap for the three different runs. For the third-order formulation, however, the rate constant estimates change significantly from run to run. Because the polyamidation rate constant should be a constant at a fixed reaction temperature rather than a function of the concentration of reactants, our data are consistent with the amidation reaction being second order, rather than third order, in the high-temperature and low-water-content conditions used in this study. The results shown in Figures 2−4 also help to explain why it was difficult for past researchers to distinguish the reaction order as either second or third order. Schaffer et al.,[2] who performed experiments at a variety of temperatures using the same end-group balance for all experimental runs, could not distinguish the reaction order for the polycondensation reaction because both assumptions produced good fits for the kinetic data. Now that we have determined that the reaction is second-order so that it is appropriate to use $X = 0$ in eqs 4 and 5, the next step is to estimate the polyamidation rate constant and the equilibrium constant using all of the available data.

## Mathematical Model

Considerable research has been devoted to describing the relationship of the apparent equilibrium constant, $K_a$, and the apparent forward rate constant, $k_p$, with temperature, water content, and end-group concentrations. Parameter estimates presented in these works are summarized in Table 2, with all symbols defined in the nomenclature. The data of Wiloth,[21,45] Ogata,[26] and Giori and Hayes[3] show that the water content in the liquid phase affects the apparent equilibrium constant significantly. Kumar et al.[46] correlated the equilibrium data of Ogata[26] using an empirical model, which is dependent on the dimensionless initial water content, $W_0$ (in moles of water per mole of initial nylon salt), in the batch reactor. However, the dependence of the correlation on the initial condition is not appropriate for studies of polyamidation in continuous industrial polymerization reactors, in which water is removed during the polymerization process.

Ogata's estimation results[26] also depend on the initial water content, assuming that $K_a$ is a constant, which is incorrect except over small ranges of temperature and water content. To overcome the above problems, Steppan et al.[12] combined the data of Ogata[26] and Giori and Hayes[3] and built an empirical equilibrium model for the whole temperature and water-content range. They also merged the high-water-content correlation of Ogata's data[26] (nylon 66) with that of Reimschuessel and Nagasubramanian[32] (nylon 6) to obtain a comprehensive reaction-rate correlation. Because nylon melt reaction systems are highly nonideal liquid solutions and the ionic character of the reaction medium can change as a result of end-group ionization, Steppan et al.[12] built an activity-based model to determine the apparent reaction equilibrium and rate constants. They proposed that, because only the rate and equilibrium constants are required, the composition dependence of the activities could be lumped into two independent groups, which

**Table 2. Literature Values of Parameters for Nylon Polycondensation[2]**

| authors | nylon type(s) | $T$, °C | water content, wt % | $B_u$, Mg mol$^{-1}$ h$^{-1}$ | $E_u$, kJ mol$^{-1}$ | $B_c$, Mg$^2$ mol$^{-2}$ h$^{-1}$ | $E_c$, kJ mol$^{-1}$ | $\Delta H$, kJ mol$^{-1}$ | $\Delta S$, kJ mol$^{-1}$ K$^{-1}$ |
|---|---|---|---|---|---|---|---|---|---|
| Fukumoto (1956) | 6 | 235−272 | 0.09−0.5 | | | | | −28.6 | $-5.75 \times 10^{-3}$ |
| Ogata (1960) | 66 | 275−300 | 0.04−0.15 | | | | | −111.1 | $-1.59 \times 10^{-1}$ |
| Ogata (1961) | 66 | 200−220 | 3.5−40.8 | exp[30.17/ $W_0^{0.025}$ − 13.82] | 92.5 | | | depends on [W] | depends on [W] |
| Giori and Hayes (1970a) | 6 and 7 | 240, 260 | 0.1−9.5 | | | | | see Figure 5.1 | see Figure 5.1 |
| Reimschuessel and Nagasubramanian (1972) | 6 | 220−265 | unknown | $8.687 \times 10^6$ | 94.4 | $2.337 \times 10^4$ | 86.5 | −25.7 | $3.89 \times 10^{-3}$ |
| Jones and White (1972) | 68 | 245−290 | unknown | $1.122 \times 10^5$ | 72.6 | | | | |
| Tai et al. (1980) | 6 | 230−280 | 1.5, 2.1 | $1.894 \times 10^7$ | 97.4 | $1.211 \times 10^4$ | 86.5 | −24.9 | $4.00 \times 10^{-3}$ |
| Tai et al. (1980) | 6 | 230−280 | 0.8 | $2.224 \times 10^7$ | 98.8 | $8.455 \times 10^1$ | 67.7 | −25.2 | $3.80 \times 10^{-3}$ |
| Roerdink and Warnier (1985) | 46 | 180−230 | 7−14 | $5.926 \times 10^5$ | 81.2 | | | 0.000 | $4.70 \times 10^{-2}$ |
| Blondel et al. (1997) | 11 and 12 | 220−310 | unknown | $1.242 \times 10^4$ | 62.7 | | | | |
| Steppan et al. (1987) | 6 and 66 | 200−265 | 0.2−40.8 | depends on [W] and [C] | 89.6 | | | depends on [W] | depends on [W] |
| Mallon and Ray (1998) | 6 and 66 | 200−280 | 0.2−40.8 | | | exp[40.72/$\epsilon RT$ − 10.19] | 35.9 | 1.7 | $5.23 \times 10^{-2}$ |
| Schaffer et al. (2003) | 612 | 263−289 | 0.03−0.15 | | | $3.34 \times 10^5$ | 94.8 | −7.62 | |

depend only on the reactant and product activities. They obtained correlations for $K_a$ and $k_p$ across broad ranges of temperatures and water concentrations, with $\Delta H$ and $\Delta S$ expressed as empirical functions of [W]. They estimated the activation energy for the uncatalyzed amidation reaction, $E_u$, to be 89.6 kJ mol$^{-1}$ and expressed the corresponding preexponential factor, $B_u$, as a function of both [W] and [C].

Some researchers[32,47,48] have used a combination of both second- and third-order kinetics, simultaneously estimating an uncatalyzed rate constant ($k_u$) and an acid-catalyzed rate constant ($k_c$), which are used to calculate a composite rate constant:

$$k_p = k_u + k_c[C] \tag{8}$$

If purely second-order kinetics are assumed, $k_c = 0$ and $k_p = k_u$, whereas if purely third-order kinetics are assumed, $k_u = 0$ and $k_p = k_c[C]$. Reimschuessel and Nagasubramanian[32] regressed the kinetic rate constant as a linear combination of these second- and third-order rate parts, with different activation energies. They also developed equilibrium correlations for nylon 6 polymerization. Their estimated values for the activation energy agree well with that of Ogata,[26] and their $\Delta H$ value agrees well with that of Fukumoto,[18] although the $\Delta S$ values do not agree, because they have opposite signs.

Tai et al.[47,48] performed nylon 6 polymerization experiments at 230−280 °C in a batch reactor with different initial water concentrations (0.42−1.18 mol kg$^{-1}$). Using the combined kinetic formulation, they estimated rate and equilibrium constants and obtained values consistent with those of Reimschuessel and Nagasubramanian.[32] The estimated parameters varied with the initial water content. The relative contribution of $k_c$ to $k_p$ in eq 8 decreases with decreasing initial water content, indicating primarily second-order kinetics at low water contents, which agree with the results of Giori and Hayes.[3]

Mallon and Ray[14] used a less empirical modeling approach to fit the literature data. They assumed that water exists in two states in nylon melts (free water and water hydrogen bonded in "bridges" between carbonyl groups) and that only free water can participate in the reversible polycondensation reaction. Mallon and Ray[14] estimated parameters for the temperature dependencies of the equilibrium constants of the hypothesized water−bridge formation reaction and the polycondensation reaction with only free water participating. Their model accounts for the experimentally observed decrease in $K_a$ with increasing total water concentration at high water concentrations because of an increase in the relative proportion of free water but does not account for a decrease in $K_a$ with decreasing water content in the low-water-content regime. The dependence of $k_p$ on the water content and the shift in the apparent kinetics from third to second order were explained by adding a reversible "salting-like" prereaction step to the polycondensation reaction. This mechanism involves ionization of acid and amine end groups, their subsequent association with each other, and reaction of the associated ion pair to form an amide link. Acid catalysis (overall third-order kinetics) was assumed under all conditions. Mallon and Ray proposed that, because the "salting-like" reaction involves charge transfer, the equilibrium constant of this reaction (and, hence, the overall rate of reaction) would decrease as the dielectric constant of

the reaction medium increases, because of increasing water content. The model of Mallon and Ray shows a good agreement with literature nylon 6 data and agrees with the rate data of Ogata[26] for nylon 66 at 220 °C slightly better than the model of Steppan et al.[12] does.

Schaffer et al.[2] studied nylon 612 polycondensation and built a mathematical model that considers polycondensation and hydrolysis reactions, as well as water mass transfer between liquid and vapor phases. The effect of the water concentration on the apparent equilibrium constant was handled using activity coefficients to relate the apparent equilibrium constant to the true thermodynamic equilibrium constant, $K_t$.

$$K_a = \frac{\gamma_C \gamma_A}{\gamma_L \gamma_W} K_t \tag{9}$$

$\gamma_A$, $\gamma_C$, $\gamma_L$, and $\gamma_W$ are activity coefficients of amine, carboxyl, amide links, and water, respectively, in the molten polymer. Schaffer et al.[2] estimated $\gamma_W$ as a function of temperature using vapor−liquid equilibrium data. They also defined the ratio of the remaining activity coefficients as an empirical linear function of the water concentration:

$$\gamma_C \gamma_A / \gamma_L = b + m[W]_{eq} \tag{10}$$

The model developed in this work builds on the approach of Schaffer et al., using the following equation to include the temperature dependence of the thermodynamic equilibrium constant:

$$K_t = \exp\left(-\frac{\Delta H}{RT} + \frac{\Delta S}{R}\right) \tag{11}$$

where $\Delta H$ is the enthalpy of reaction, $\Delta S$ is the change of entropy, and $R$ is the ideal gas law constant.

As a result, the temperature and composition dependencies of the apparent equilibrium constant can be expressed as

$$K_a = \frac{[L]_{eq}[W]_{eq}}{[A]_{eq}[C]_{eq}} = \frac{\gamma_A \gamma_C}{\gamma_L \gamma_W} K_t = \frac{\gamma_A \gamma_C}{\gamma_L \gamma_W} \exp\left(\frac{-\Delta H}{RT} + \frac{\Delta S}{R}\right) \tag{12}$$

For experimental conditions in which the water content in the nylon 612 melt is low, Schaffer et al.'s Flory−Huggins-based model[43] can be used to calculate $\gamma_W$:

$$\gamma_W = \exp\left(9.624 - \frac{3613}{T}\right) \tag{13}$$

Because $\gamma_W$ is a function of temperature, it is reasonable to expect that $\gamma_A\gamma_C/\gamma_L$ will also be temperature-dependent. The following empirical expression (an improved version of eq 10) was developed to include the influence of both temperature and moisture content on the activity coefficient ratio:

$$\gamma_A \gamma_C / \gamma_L = b + m \exp(\beta/T)[W]_{eq} \tag{14}$$

When eqs 11 and 14 are substituted into eq 12, the apparent equilibrium constant is expressed as

$$K_a = \left[\frac{b + m \exp(\beta/T)[W]_{eq}}{\gamma_W}\right] \exp\left(-\frac{\Delta H}{RT} + \frac{\Delta S}{R}\right) \tag{15}$$

To reduce the number of parameters, as well as the correlation between the estimated model parameters, eq 15 was rearranged to a form involving a reference temperature, $T_0$, and a reference value of the apparent equilibrium constant, $K_{a0}$, the value of the apparent equilibrium constant at temperature $T_0$, under low-moisture conditions, where $[W]_{eq} \rightarrow 0$:

$$K_a = \left[\frac{1 + \exp(\alpha + \beta/T)[W]_{eq}}{\gamma_W/\gamma_{W0}}\right] K_{a0} \exp\left[-\frac{\Delta H}{R}\left(\frac{1}{T} - \frac{1}{T_0}\right)\right] \tag{16}$$

where eq 16 is related to eq 15 by $\alpha = \ln(m/b)$ and

$$K_{a0} = \left(\frac{b}{\gamma_{W0}}\right) \exp\left(-\frac{\Delta H}{RT_0} + \frac{\Delta S}{R}\right)$$

The reference temperature that was selected is $T_0 = 549$ K, which is the middle of the temperature range used in Schaffer et al.'s study[2] of the effects of temperature on polycondensation. $\gamma_{W0}$ is the water activity coefficient at $T_0$, which was calculated from eq 13 to give $\gamma_{W0} = 20.97$. $\alpha$ and $\beta$ are empirical parameters that need to be estimated. The temperature dependence of the polycondensation rate constant, $k_p$, can be described using a centered Arrhenius expression:

$$k_p = k_{p0} \exp\left[-\frac{E}{R}\left(\frac{1}{T} - \frac{1}{T_0}\right)\right] \tag{17}$$

where $k_{p0}$ is the rate constant at reference temperature $T_0$.

## Parameter Estimation and Simulation Results

The model developed in the last section (eqs 2−6, 13, 16, and 17) has six unknown parameters: $k_{p0}$, $E$, $K_{a0}$, $\Delta H$, $\alpha$, and $\beta$. The experimental data of Schaffer et al.[2] and new data from the present study were combined to estimate these parameters. The initial values for all six parameters are required so that weighted nonlinear least-squares regression can be used. Fortunately, we were able to obtain reasonable initial values by dividing the parameters into three pairs ($\alpha$ and $\beta$, $K_{a0}$ and $\Delta H$, and $k_{p0}$ and $E$) and estimating the three pairs of parameters, one pair at a time, using subsets of the available data. Finally, all of the data were used together to refine the parameter estimates.

For each experimental temperature used by Schaffer et al.,[2] steady-state data are available for two water concentration levels, a pure steam atmosphere and mostly $N_2$ (80 mol % $N_2$/20 mol % steam). Using eq 16, at a specified temperature, the ratio of the apparent equilibrium constants at the high- and low-water-content conditions, $K_{aH}/K_{aL}$, is

$$\frac{K_{aH}}{K_{aL}} = \frac{1 + \exp(\alpha + \beta/T)[W]_{eqH}}{1 + \exp(\alpha + \beta/T)[W]_{eqL}} \tag{18}$$

When eq 18 is rearranged, the following equation can be obtained:

$$\frac{K_{aH} - K_{aL}}{K_{aL}[W]_{eqH} - K_{aH}[W]_{eqL}} = \exp(\alpha + \beta/T) \tag{19}$$

The apparent equilibrium constants at high water content, $K_{aH}$, and at low water content, $K_{aL}$, on the left-

**Table 3. Parameter Estimates**

| param | units | initial estimate | refined estimate | 95% CI (±) |
|---|---|---|---|---|
| $k_{p0}$ | Mg mol$^{-1}$ h$^{-1}$ | $1.77 \times 10^{-2}$ | $1.91 \times 10^{-2}$ | $0.2034 \times 10^{-2}$ |
| $E$ | kJ mol$^{-1}$ | 28.2712 | 45.904 | 32.354 |
| α | exp(α) in Mg mol$^{-1}$ | 23.8356 | 22.6039 | 13.215 |
| $\beta$ | $K$ | $-1.5183 \times 10^{4}$ | $-1.4468 \times 10^{4}$ | $0.7304 \times 10^{4}$ |
| $K_{a0}$ | dimensionless | 57.3685 | 53.7841 | 4.95 |
| $\Delta H$ | kJ mol$^{-1}$ | −78.069 | −85.752 | 26.434 |

hand side of eq 19 can be calculated from the steady-state experimental data, and the equilibrium water contents at different moisture levels can be calculated from eqs 2 and 3. Natural logarithms were taken of both sides of eq 19 so that linear regression could be used to obtain the initial estimates of α and $\beta$. The results are shown in the initial estimate column of Table 3. The initial estimates of α and $\beta$ were substituted into eq 16, before taking the natural logarithms of both sides of the equation. Linear regression was then used to estimate the initial values of the parameters $K_{a0}$ and $\Delta H$ (shown in Table 3).

Experimental data at different temperatures, and the dynamic model, were then used to estimate the apparent rate constant of the polycondensation reaction at each temperature, using weighted nonlinear least-squares estimation. Previously determined initial values for α, $\beta$, $K_{a0}$, and $\Delta H$ were used to calculate $K_a$ from eq 16. After $k_p$ was determined for each temperature, linear regression was performed using natural logarithms of both sides of eq 17 so that the initial estimates for parameters $k_{p0}$ and $E$ could be determined from the slope and intercept. The results are shown in Table 3.

Using the initial parameter values in Table 3 and weighted nonlinear least-squares regression, the parameters were reestimated using the "lsqnonlin" Matlab routine. The refined parameter estimation results are also shown in Table 3. The parameter estimation results indicate that the polycondensation reaction is exothermic because of the negative sign of the heat of reaction, $\Delta H$, which agrees with most literature results. The value of the reaction enthalpy from the present study is close to that in other low-water-content studies but is much smaller than $\Delta H$ from studies with high water contents. The difference in $\Delta H$ between high- and low-water-content conditions[12] has been attributed to ionization reactions. Therefore, the equilibrium constant that is estimated from this study should only be used for predicting heat effects and the reaction equilibrium in the low-water-content region. The value of the estimated activation energy is close to the literature data in Table 2.

Using the present model and the estimated parameters, experimental data obtained using different reactor temperatures and end-group balances were simulated. The results are shown in Figures 5−10. The simulation curves follow the experimental data quite well and agree more closely with the [A] data than with the [C] data, as was anticipated as a result of using the more precise [A] measurements and the corresponding weighting factors used in the estimation procedure.

**Effects of End-Group Balance.** The present experimental data indicate that changing the end-group balance does not affect the apparent equilibrium constant of the polycondensation reaction. This result agrees with the results of Heikens et al.,[17] who found that the value of the apparent equilibrium constant of the polycondensation reaction is not affected by the presence of an excess of either amine or carboxyl end groups. However, this result does not support Mallon and Ray's assumption[14] that the water exists in two states in nylon melts and only free water can participate in the polycondensation reaction. On the basis of their assumption, adding more carboxyl end groups or adding more amine end groups would increase or reduce the amount of water hydrogen bonded in "bridges" between carbonyl groups, which would either decrease or in-

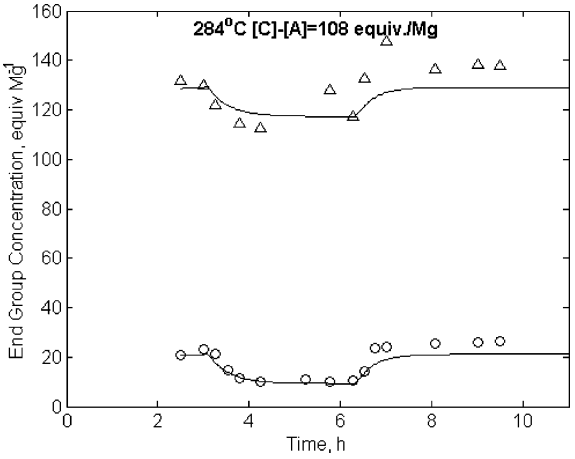


**Figure 5.** Simulation results of end-group data for run at 284 °C with [C] − [A] =108 mol Mg$^{-1}$: (△) measured [C]; (○) measured [A]; (—) model.

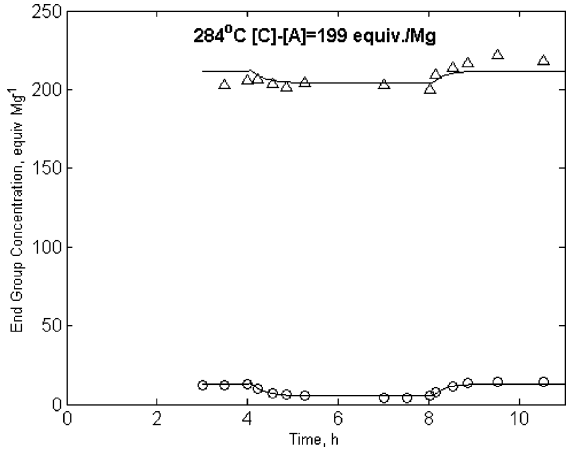


**Figure 6.** Simulation results of end-group data for run at 284 °C with [C] − [A] = 199 mol Mg$^{-1}$: (△) measured [C]; (○) measured [A]; (—) model.

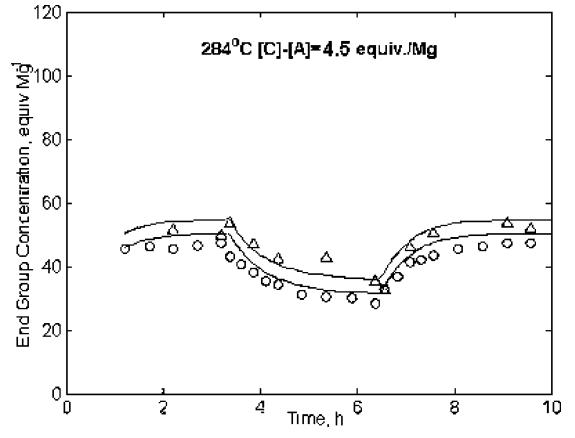


**Figure 7.** Simulation results of end-group data for run at 284 °C with [C] − [A] = 4.5 mol Mg$^{-1}$: (△) measured [C]; (○) measured [A]; (—) model.

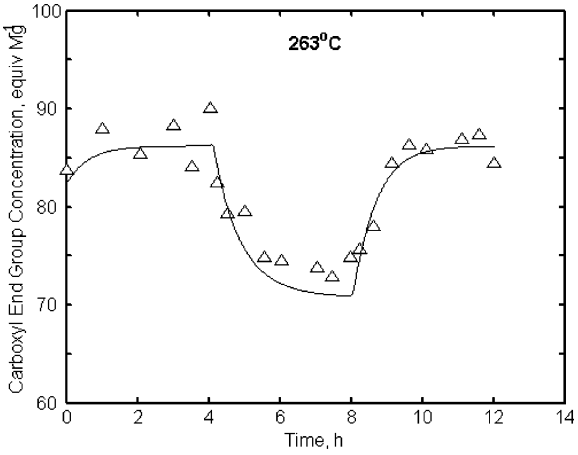


(a) Carboxyl End-Group

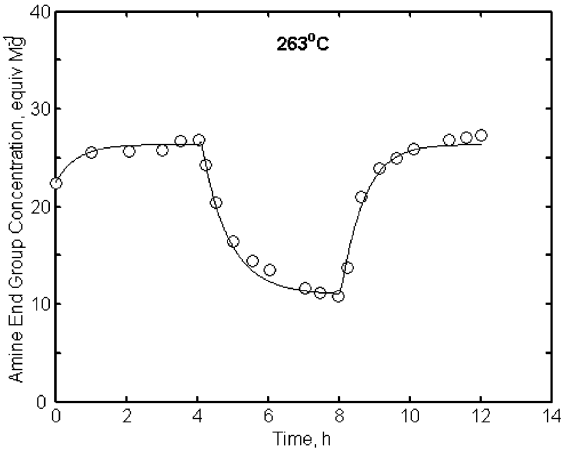


(b) Amine End-Group

**Figure 8.** Simulation results of end-group data run at 263 °C: (△) measured [C]; (○) measured [A]; (—) model.

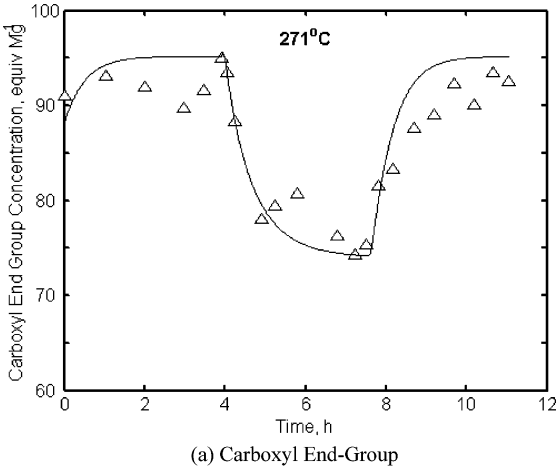


(a) Carboxyl End-Group

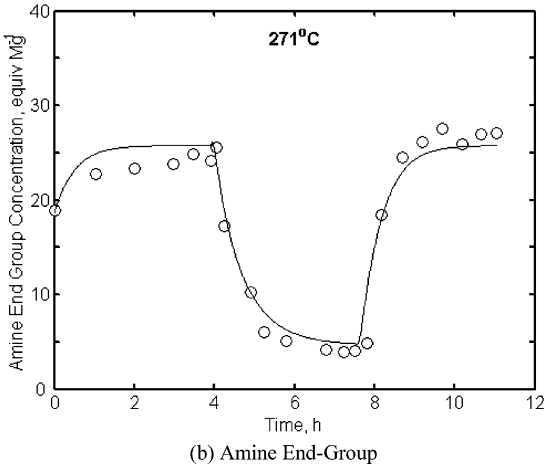


(b) Amine End-Group

**Figure 9.** Simulation results of end-group data run at 271 °C: (△) measured [C]; (○) measured [A]; (—) model.

crease the concentration of free water. If only the free water can participate in the polycondensation and hydrolysis reactions, the apparent equilibrium constant should be changed with a change in the end-group balance, but the experimental data do not show this.

**Effect of the Water Content on the Apparent Equilibrium Constant.** The apparent equilibrium constant, $K_a$, decreases with decreasing water content in the melt phase of the polymer, in the low-water-content region explored in this study. For example, parameter estimates indicate that when the moisture content in the melt changes from 0.02 to 0.07 wt % at a temperature of 284 °C, $K_a$ changes from 50 to 74. This result agrees with the data of Giori and Hayes[3] but disagrees with those of some other researchers,[11] who claimed that $K_a$ is constant at low water concentrations rather than decreasing with decreasing water content. Because the weight of evidence is that the water content is an important factor for calculating the apparent equilibrium constant, activity coefficient terms that account for changing the water concentration have been included in the present model.

**Enthalpy.** $\Delta H$ for polyamidation reactions is known to depend on [W][12] so that the estimated value of enthalpy from this study can only be used in the low water concentration range. Estimation of the enthalpy of the ionization and polyamidation reactions separately could be used to solve this problem. However, this would not be straightforward because of the fundamental difficulty of distinguishing between the ionic and molecular species involved in the preceding reaction schemes. The values for the reactant concentration terms in equilibrium and other polyamidation kinetic equations have been measured by amine and carboxyl end-group titration. Because both ionized and nonionized end-group species are consumed during titration, measurements of the individual concentrations of the ionized and nonionized end groups in the reacting mixture cannot be determined using this method. Because amine and carboxyl end groups in some of their forms (e.g., ionized or nonionized) may not participate directly in the polycondensation reaction, the kinetic and equilibrium data obtained here, and in other polyamidation equilibrium and kinetic studies, are apparent values that are appropriate for the composite ionization and polyamidation reactions. This simplified approach provides a useful basis for predicting the macroscopic dependence of polyamide equilibrium and reaction rates upon changes in key reaction variables, including temperature and end-group and water concentrations, over the limited but important range of the study.

## Summary

This study examines the effects of end-group balance on the kinetics and equilibrium of nylon 612 polycondensation reactions at high temperatures and low water concentrations (<0.002 weight fraction). Three experimental runs at 284 °C, with different end-group bal-

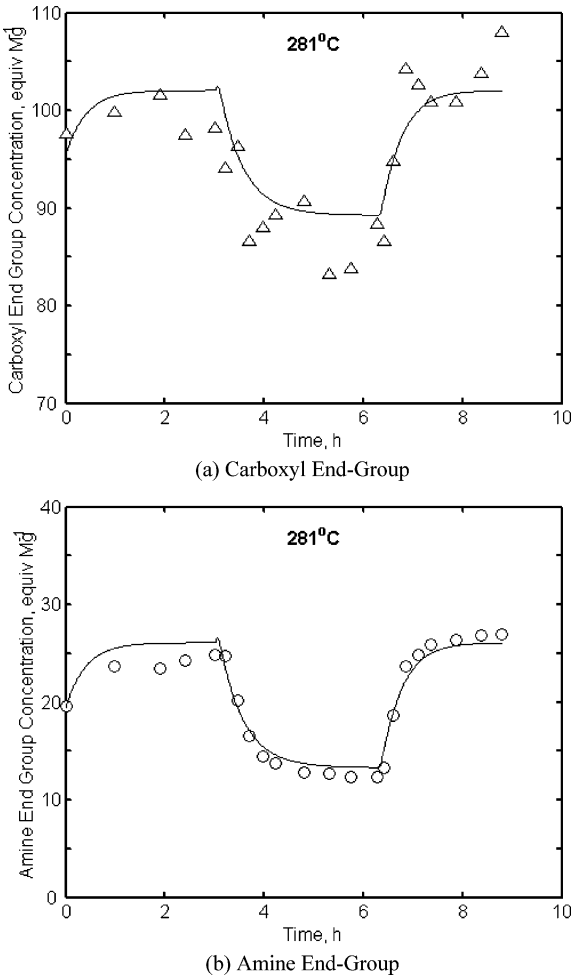


**Figure 10.** Simulation results of end-group data run at 281 °C: (△) measured [C]; (○) measured [A]; (—) model.

ances and time-varying moisture levels, were used to demonstrate that the kinetic order of the polycondensation reaction is much closer to second-order than third-order in this operating region.

A mathematical model was developed to describe the effects of temperature and end-group and water concentrations on the rates of polyamidation and hydrolysis reactions. The effect of the water concentration on the apparent equilibrium constant was described semiempirically by expressing the ratio of the end-group and amide link activity coefficients as functions of temperature and equilibrium water concentration. The observed variation of $K_a$ with the water content indicates that it is necessary and advisable to include the effect of the water content on the apparent equilibrium constant so that polycondensation reaction kinetics and equilibrium can be accurately predicted. Estimates of the model parameters are in order-of-magnitude agreement with literature values from earlier polyamidation studies, and simulation results match the isothermal experimental data obtained in this study, as well as data obtained from an earlier set of nonisothermal experiments conducted by Schaffer et al.[2] The new experimental data and the proposed mathematical model should prove useful for simulation of industrial processes for melt-phase nylon polycondensation in various reactor configurations and will aid in the design of process improvements for the final stages of nylon production.

## Acknowledgment

The authors are grateful for the financial support provided by NSERC, DuPont Canada, and Queen's University.

## Nomenclature

[A] = concentration of amine end groups, mol $Mg^{-1}$
[Â] = calculated concentration of amine end groups, mol $Mg^{-1}$
$b$ = empirical parameter used by Schaffer et al.[2] in the empirical activity coefficient ratio model
$B_u$, $B_c$ = Arrhenius preexponential factor for uncatalyzed (second-order) and catalyzed (third-order) polyamidation, Mg $mol^{-1}$ $h^{-1}$ and $Mg^2$ $mol^{-2}$ $h^{-1}$, respectively
[C] = concentration of carboxylic acid end groups, mol $Mg^{-1}$
[Ĉ] = calculated concentration of carboxylic acid end groups, mol $Mg^{-1}$
$E$ = activation energy, kJ $mol^{-1}$
$E_u$, $E_c$ = activation energy for uncatalyzed (second-order) and catalyzed (third-order) polyamidation, kJ $mol^{-1}$
$\Delta H$ = apparent enthalpy of polycondensation, kJ $mol^{-1}$
[L] = concentration of amide links, mol $Mg^{-1}$
$J$ = objective function for weighted nonlinear regression
$K_a$ = apparent polycondensation equilibrium constant
$K_{a0}$ = apparent polycondensation equilibrium constant at $T_0$ and very low water content
$k_m$ = volumetric liquid-phase mass-transfer coefficient for a nylon/water system, $h^{-1}$
$k_p$ = apparent polycondensation rate constant, Mg $mol^{-1}$ $h^{-1}$
$k_{p0}$ = apparent polycondensation rate constant at reference temperature 549.15 K
$k_u$, $k_c$ = polycondensation rate constants for uncatalyzed (second-order) and catalyzed (third-order) kinetics, Mg $mol^{-1}$ $h^{-1}$ and $Mg^2$ $mol^{-2}$ $h^{-1}$, respectively
$K_t$ = thermodynamic polycondensation equilibrium constant
$m$ = empirical parameter used by Schaffer et al.[2] in the empirical activity coefficient ratio model, Mg $mol^{-1}$
$n_A$ = number of amine end-group samples
$n_C$ = number of carboxyl end-group samples
$P_c$ = critical pressure of water, kPa
$P_w$ = partial pressure of water in the gas phase, kPa
$P_w^{sat}$ = saturation pressure of water in the gas phase, kPa
$R$ = ideal gas law constant, $8.3145 \times 10^{-3}$ kJ $mol^{-1}$ $K^{-1}$
$\Delta S$ = apparent entropy of polycondensation, kJ $mol^{-1}$ $K^{-1}$
$t$ = time, h
$T$ = temperature, K
$T_0$ = reference temperature, 549.15 K
$T_c$ = critical temperature of water, K
[W] = concentration of water, mol $Mg^{-1}$
$W_0$ = ratio of moles of initial water to moles of initial nylon salt, used by Ogata
$X$ = exponent in the kinetic expression for the reaction rate

*Greek Letters*

$\alpha$ = empirical model parameter, $\exp(\alpha)$ has units of Mg $mol^{-1}$
$\beta$ = empirical model parameter to predict the effect of $T$ on the activity coefficient ratio, K
$\gamma_i$ = activity coefficient of species $i$
$\sigma_A$, $\sigma_C$ = standard deviations of amine and carboxyl end-group measurements, mol $Mg^{-1}$

## Literature Cited

(1) Schaffer, M. A. Chemical Pathways and Kinetics of the Later Stages of Nylon Polymerization Processes. Ph.D. Thesis, Queen's University, Kingston, Ontario, Canada, 2003.

(2) Schaffer, M. A.; McAuley, K. B.; Cunningham, M. F.; Marchildon, E. K. Experimental Study and Modeling of Nylon Polycondensation in the Melt Phase. *Ind. Eng. Chem. Res.* **2003**, *42*, 2946.

(3) Giori, C.; Hayes, B. T. Hydrolytic Polymerization of Caprolactam. I. Hydrolysis−Polycondensation Kinetics. *J. Polym. Sci., Polym. Chem. Ed.* **1970**, *8*, 335.

(4) Ogata, N. Studies on Polycondensation Reactions of Nylon Salt. II. The Rate of Polycondensation Reaction of Nylon 66 Salt in the Presence of Water. *Makromol. Chem.* **1961**, *43*, 117.

(5) Jones, D. C.; White, T. R. Polyamides. In *Step-Growth Polymerizations*; Solomon, D. H., Ed.; Kinetics and Mechanisms of Polymerization Series; Marcel Dekker: New York, 1972; Vol. 3, p 41.

(6) Roerdink, E.; de Jong, P. J.; Warnier, J. Study on the Polycondensation Kinetics of Nylon-4,6 Salt. *Polym. Commun.* **1984**, *25*, 194.

(7) Roerdink, E.; Warnier, J. M. M. Preparation and Properties of High Molar Mass Nylon-4,6: A New Development in Nylon Polymers. *Polymer* **1985**, *26*, 1582.

(8) Blondel, P.; Briffaud, T.; Werth, M. R. G. Kinetics of Polycondensation in an Industrial Environment. *Macromol. Symp.* **1997**, *122*, 243.

(9) Pagilagan, R. U. Chemistry. In *Nylon Plastics Handbook*; Kohan, M. I., Ed.; Hanser/Gardner: Cincinnati, OH, 1995; p 33.

(10) Miller, I. K.; Zimmerman, J. Condensation Polymerization and Polymerization Mechanisms. In *Applied Polymer Science*, 2nd ed.; Tess, R. W., Poehlein, G. W., Eds.; ACS Symosium Series 285; American Chemical Society: Washington, DC, 1985; p 166.

(11) Zimmerman, J. Polyamides. In *Encyclopedia of Polymer Science and Engineering*, 2nd ed.; Mark, H. F., Kroschwitz, J. I., Eds.; Wiley: New York, 1988; Vol. 11, p 329.

(12) Steppan, D. D.; Doherty, M. F.; Malone, M. F. A Kinetic and Equilibrium Model for Nylon 6,6 Polymerization. *J. Appl. Polym. Sci.* **1987**, *33*, 2333.

(13) Kohan, M. I. Polyamides. In *Ullmann's Encyclopedia of Industrial Chemistry*, 5th ed.; Campbell, T., Pfefferkorn, R., Rounsaville, J. F., Eds.; VCH Publishers: New York, 1992; Vol. A21, p 179.

(14) Mallon, F. K.; Ray, W. H. A Comprehensive Model for Nylon Melt Equilibria and Kinetics. *J. Appl. Polym. Sci.* **1998**, *69*, 1213.

(15) Hermans, P. H. Chemistry of Caprolactam Polymerization. *J. Appl. Chem.* **1955**, *5*, 493.

(16) Hermans, P. H.; Heikens, D.; van Velden, P. F. On the Mechanism of the Polymerization of ϵ-Caprolactam. II. The Polymerization in the Presence of Water. *J. Polym. Sci.* **1958**, *30*, 81.

(17) Heikens, D.; Hermans, P. H.; van der Want, G. M. On the Mechanism of the Polymerization of ϵ-Caprolactam. IV. Polymerization in the Presence of Water and Either an Amine or a Carboxylic Acid. *J. Polym. Sci.* **1960**, *44*, 437.

(18) Fukumoto, O. Equilibria between Polycapramide and Water. I. *J. Polym. Sci.* **1956**, *22*, 263.

(19) Wiloth, F. Uber den Mechanismus und die Kinetik der ϵ-Caprolactam Polymerisation in Gegenwart von Wasser. 2. Uber das Kondensationsgleichgewicht bei Polyamiden, eine Modelluntersuchung (About the mechanism and the kinetics of ϵ-caprolactam polymerization in the presence of water. 2. The condensation equilibrium of polyamides, a case study). *Makromol. Chem.* **1955**, *15*, 98.

(20) Wiloth, F. Uber den Mechanismus und die Kinetik der ϵ-Caprolactam Polymerisation in Gegenwart von Wasser. 4. Das Gleichgewicht des Systems ϵ-Caprolactam−Poly-ϵ-Caprolactam−Wasser bei 220° (About the mechanism and the kinetics of ϵ-caprolactam polymerization in the presence of water. 4. The equilibrium of the system ϵ-caprolactam/poly-ϵ-caprolactam/water at 220°). *Z. Phys. Chem. (Munich), N.F.* **1955**, *4*, 66.

(21) Wiloth, F. Uber den Mechanismus und die Kinetik der ϵ-Caprolactam Polymerisation in Gegenwart von Wasser. 5. Messungen zur Kinetik der Bildung des Poly-ϵ-Caprolactam in neutralem Medium (About the mechanism and the kinetics of ϵ-caprolactam polymerization in the presence of water. 5. Measuring the kinetics of the formation of poly-ϵ-caprolactam in neutral medium). *Kolloid Z.* **1955**, *143*, 129.

(22) Giori, C.; Hayes, B. T. Hydrolytic Polymerization of Caprolactam. II. Vapor−Liquid Equilibria. *J. Polym. Sci., Polym. Chem. Ed.* **1970**, *8*, 351.

(23) Wiloth, F. Uber Den Mechanismus und die Kinetik der Caprolactam-Polymerisation in Gegenwart von Wasser. 15. Anmerkung zu neueren MeBwerten ubder die Gleichgewichtskonstante der Polykondensation (About the mechanism and the kinetics of ϵ-caprolactam polymerization in the presence of water. 15. Note on new data for the equilibrium constants for polycondensation). *Makromol. Chem.* **1971**, *144*, 329.

(24) Tai, K.; Teranishi, H.; Arai, Y.; Tagawa, T. The Kinetics of Hydrolytic Polymerization of ϵ-Caprolactam. *J. Appl. Polym. Sci.* **1979**, *24*, 211.

(25) Ogata, N. Studies on Polycondensation Reactions of Nylon Salt. I. The Equilibrium in the System of Polyhexamethylene Adipamide and Water. *Makromol. Chem.* **1960**, *42*, 52.

(26) Ogata, N. Studies on Polycondensation Reactions of Nylon Salt. II. The Rate of Polycondensation Reaction of Nylon 66 Salt in the Presence of Water. *Makromol. Chem.* **1961**, *43*, 117.

(27) Schaffer, M. A.; Marchildon, E. K.; McAuley, K. B.; Cunningham, M. F. Thermal Non-oxidative Degradation of Nylon 6,6. *J. Macromol. Sci. Rev.* **2000**, *C40*, 233.

(28) Bailey, W. J. Thermal decomposition of unsaturated materials. *Polym. Eng. Sci.* **1965**, 5, 59.

(29) Wiloth, F.; Schindler, E. Decarboxylation of β-oxo acid amides. *Chem. Ber.* **1967**, *100*, 2373.

(30) Wiloth, F.; Schindler, E. Thermal degradation of nylon 66. II. Thermolysis of *N*-*n*-hexyl-2-(*n*-hexylimino)cyclopentane-1-carboxamide. Elimination of isocyanate from ϵ-carbamoylcyclopentanone imines. *Chem. Ber.* **1970**, *103*, 757.

(31) Gaymans, R. J.; Sikkema, D. J. Aliphatic Polyamides. In *Step Polymerization*; Allen, G., Bevington, J. C., Eds.; Comprehensive Polymer Science Series; Pergamon Press: Oxford, U.K., 1989; Vol. 5, p 357.

(32) Reimschuessel, H. K. Nagasubramanian, K. On the Optimization of Caprolactam Polymerization. *Chem. Eng. Sci.* **1972**, *27*, 1119.

(33) Pinney, B. M. High Viscosity Finisher. U.S. Patent 3,717,-330, 1973.

(34) Iwasyk, J. M. Apparatus for Finishing High Viscosity Synthetic Polymers. U.S. Patent 4,090,261, 1978.

(35) Kendall, J. A.; Marchildon, E. K.; Stephenson, G. R. Self-wiping Multiple Screw Element Mixer. U.S. Patent 4,344,711, 1982.

(36) Livingston, R. D. Apparatus for Finishing Synthetic Polymers. U.S. Patent 4,370,061, 1983.

(37) Schaffer, M. A.; Marchildon, E. K.; McAuley, K. B.; Cunningham, M. F. Assessment of Mixing Performance and Power Consumption of a Novel Polymerization System. *Chem. Eng. Technol.* **2001**, *24*, 401

(38) Sibila, J. P.; Murthy, N. S.; Gabriel, M. K.; McDonnell, M. E.; Bray, R. G.; Curran, S. A. Characterization. In *Nylon Plastics Handbook*; Kohan, M. I., Ed.; Hanser/Gardner: Cincinnati, OH, 1995; pp 70−83.

(39) Meacock, G. Production of Fibres from 6,6-, 6,10- and 6-Polyamides. *J. Appl. Chem.* **1954**, *4*, 172.

(40) Wiloth, F. Zur Thermischen Zersetzung von Nylon 66 (On the thermal degradation of nylon 66). *Makromol. Chem.* **1971**, *144*, 283.

(41) Peebles, L. H.; Huffman, M. W. Thermal Degradation of Nylon 66. *J. Polym. Sci., Polym. Chem. Ed.* **1971**, *9*, 1807.

(42) Yoshizawa, Y.; Saito, H.; Nukada, K. Direct observation of the crosslinking unit in thermally degraded polyamides. *J. Polym. Sci., Part B: Polym. Lett.* **1972**, *10*, 145.

(43) Schaffer, M. A.; Marchildon, E. K.; McAuley, K. B.; Cunningham, M. F. Prediction of Water Solubility in Nylon Melts Based on Flory−Huggins Theory. *Polym. Eng. Sci.* **2003**, *43*, 639.

(44) Poling, B. E.; Prausnitz, J. M.; O'Connell, J. P. *The Property of Gas and Liquids*, 5th ed.; McGraw-Hill: New York, 2001; Chapter 7.

(45) Wiloth, F. The mechanism and kinetics of ϵ-caprolactam polymerization in the presence of water. III. Influence of water on the formation of poly-ϵ-caprolactam. *Makromol. Chem.* **1955**, *15*, 106.

(46) Kumar, A.; Kuruville, S.; Raman, A. R.; Gupta, S. K. Simulation of Reversible Nylon 66 Polymerization. *Polymer* **1981**, *22*, 387.

(47) Tai, K.; Teranishi, H.; Arai, Y.; Tagawa, T. The Kinetics of Hydrolytic Polymerization of ϵ-Caprolactam II: Determination

of the Kinetic and Thermodynamic Constants by Least-Squares Curve Fitting. *J. Appl. Polym. Sci.* **1980**, *25*, 77.

(48) Tai, K.; Teranishi, H.; Arai, Y.; Tagawa, T. The kinetics of hydrolytic polymerization of $\epsilon$-caprolactam. *J. Appl. Polym. Sci.* **1979**, *24*, 211.

*Received for review* June 16, 2004
*Revised manuscript received* September 29, 2004
*Accepted* September 30, 2004

IE049474N